Indian J Phys (December 2019) 93(12):1619–1624
https://doi.org/10.1007/s12648-019-01419-5

ORIGINAL PAPER

Ablation of silicon and ultrathin fibers using single femtosecond pulse

M S Sidhu* and K P Singh

Department of Physical Sciences, Indian Institute of Science Education and Research Mohali, Sector-81, Manauli 140306, India

Received: 15 April 2018 / Accepted: 11 January 2019 / Published online: 28 March 2019

Abstract: We exploit the nonlinear multiphoton interaction of a few-cycle femtosecond (fs) pulse with viscoelastic microfibers in order to produce nanoscale grooves on its surface. The single fs pulse has been extracted from 1 kHz pulse train by double-shutter gating technique by placing two mechanical shutters in the beamline and simultaneously triggering them with a controlled delay. With adjustment of the time delay between two shutters, a small transmission window has been created to cleanly extract a single or desired number of pulses. We found that the single-pulse ablation threshold for microfiber is 1 J/cm ^{2} while for absorbing surfaces like crystalline Si is 0.01 J/cm^2. Precise diffraction unlimited ablation of materials opens a route to process nanoscale waveguides, microfluidic devices to isolate cells or macro-molecules.

Keywords: Ultrafast lasers; Silicon; Silk; Femtosecond laser

PACS Nos.: 07.60.j Optical instruments and equipment; 42.65.Re Ultrafast processes; optical pulse generation and pulse compression; 06.60.Jn High-speed techniques (microsecond to femtosecond)

1. Introduction

Nonlinear interaction of femtosecond (fs) pulses with materials have diverse applications such as studying ultrafast dynamics of matter [1], precision material processing [2, 3], generation of XUV pulses [4, 5], time-resolved imaging [6] and ultrafast spectroscopy [7]. Generally, most strong field experiments are performed with a fs pulse train, typically at kHz repetition rate, and their short interaction times, when compared to other physical processes, reveal underlying fs response of materials [8–10]. The fs ablation of dielectrics and semiconductors is experimentally well established along with its theoretical understanding [2, 3]. The intense fs pulse is absorbed via multiphoton absorption by electrons at fs time scale, referred to as 'carrier-excitation,' followed by carrier-phonon scattering where electrons dissipate energy to the lattice. This raises the lattice temperature nonlinearly in ps to sub-ns time scales, resulting in ultrafast melting and material removal due to the expansion of hot matter[2, 3, 11]. These mechanisms allow precise ablation of material, not limited by the diffraction limit, reaching sub-100 nm dimensions [12]. However, clean ablation of microfibers, viscoelastics and solid crystalline surfaces using single fs pulse is not easy to perform due to difficulty in extracting a single fs pulse from the pulse train and diffraction-limited focusing on 1–2 micron samples.

Previously, several methods including pulse picker or pockel cell-based techniques allow the extraction of a single pulse from a MHz–GHz pulse train [5, 13]. However, due to dispersion and low damage threshold of birefringent crystals, these methods are not suitable for (broadband) few-cycle laser pulses having high peak powers [14]. Alternatively, the single-shot response of materials was studied by rapidly scanning the sample (typically $\sim$ 10 mm/s) in the focal plane so that the individual pulses are spatially well separated [15].It is effective for large-area flat surfaces, but may not be feasible for microfibers and microscopic (biological) samples [16].

A single mechanical shutter is commonly used to extract fs pulses by chopping the laser beam [17]. Several shutters are available that work on different actuation mechanisms such as slow thermal expansion [18–24] or piezo-mounted slits [25] and electro-mechanical actuation [26]. Previously, two shutters are used in series with a pockel cell to enhance the pulse contrast ratio for quasi-CW lasers and electron accelerators [27]. The mechanical shutters also play a vital role in isolation of XUV or electron pulses at

*Corresponding author, E-mail: sidhums@iisermohali.ac.in

synchrotron sources in time-resolved scattering or diffraction experiments [28, 29, 32]. However, the total opening times of readily available electro-mechanical shutters are typically around 2.5–60 ms (see Table 1) which fall a bit short to cleanly isolate single fs pulse from a 1 kHz pulse train. In order to perform diverse single-shot fs experiments, it has been a long-standing problem to find a simple technique that can cleanly isolate a single fs pulse from a kHz pulse train.

Here, we cleanly extract a single or desired number of fs pulses in a controlled way from a fs pulse train using a simple double-shutter gating (DSG) technique. We demonstrate single-pulse ablation of the crystalline silicon surface and quantify its crater size at different pulse energies, as well as by varying the number of pulses. With a single fs pulse exposure, we performed the nonlinear nanoscale ablation of strong and transparent spider silk fiber as a function of incident pulse energy and determined its ablation threshold. We also studied the slow transient response of a viscoelastic material, such as agarose gel, following irradiation of a single fs pulse. Agarose gel has been used as a vascular tissue model "phantom" to study the viability of short laser pulses to treat skin birthmarks such as port wine stains [30]. Furthermore, nonlinear interaction of fs pulses with microfibers along with DSG technique can also be potentially implemented in a vacuum for isolating single fs pulse of electrons or XUV light for diverse applications.

2. Operating principle of DSG

The operating principle of double-shutter gating technique is illustrated in Fig. 1(a). Two shutters, *S*1 and *S*2, are placed collinearly in the path of a pulsed fs laser beam. Initially, the shutter *S*1 is fully open, while *S*2 is fully closed. This configuration does not allow any pulse to pass through. When both the shutters are triggered in order to invert their positions, i.e., *S*1 is opening, while almost simultaneously *S*2 is closing. This operation generated an AND-gated transmission window when both the shutters

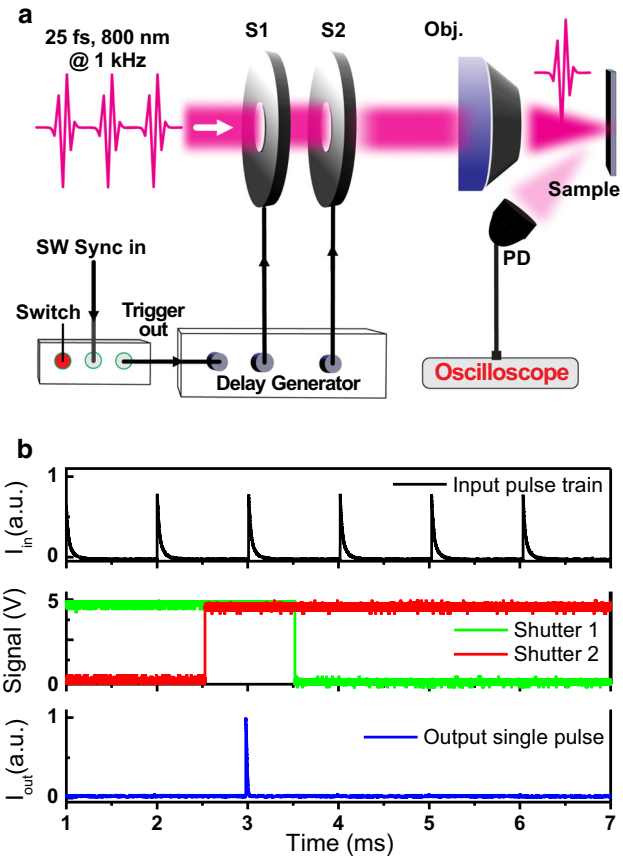

Fig. 1 (**a**) Schematics of the double-shutter gating setup. The isolated pulses were focused on a sample through a microscope objective. (**b**) Electronic photodiode signals showing input femtosecond pulse train, driving signals for the shutters and selected single output pulse. A time delay between S1 and S2 is visible that provides AND-gated transmission window adjusted using delay (SRS) generator. The shutters were synchronized with 1 kHz repetition rate (SW sync in). *S*1, *S*2: Mechanical Shutters (Vincent Tech. USA), Obj: 20× Objective (NA 0.2), *PD* Photodiode

Table 1 Comparison of commercial shutters with double-shutter gating technique. Definitions of different times are illustrated below [18]

Sr. no.	Shutter specifications	D (mm)	~Switching times (ms)	~Min. dwell time (ms)	~Min. exposure time (ms)
1.	04SMS001 (Melles Griot, USA)	11.2	–	60	60
2.	Optical beam shutter (ThorLabs, USA)	25.4	9–10	19	37
3.	Optical beam shutter (ThorLabs, USA)	12.7	3–4	10	17
4.	SR 470 (SRS, USA)	3.0	0.5	5.0	6.0
5.	10FBS-5-10 (Standa, Lithuania)	10.0	1–2	2	3
6.	Ls6 (Vincent tech. USA)	6.0	0.7–0.8	0.8	2.5
7.	Dual mechanical shutter system (this work)	6.0	0	1	1

(–) = Data not available, D = Incident beam diameter

are simultaneously open for a small time interval τ_{open}, which allows the pulses to pass through. After both the shutters have fully flipped their positions, with $S1$ close and $S2$ open, the laser beam is again blocked. By controlling the relative time delay between opening and closing of $S1$ and $S2$, the τ_{open} can be tuned to become sufficiently less than the inter-pulse period. In addition, the transmission window must be synchronized with the pulses by triggering the shutters with the input pulse train. This allows only single fs pulse to pass through the double-shutter system despite the slow on–off cycle of a single shutter.

3. Methods

Schematic diagram of the setup is shown in Fig. 1(a). We used a collimated fs laser beam having $1/e^2$ full waist of about 12 mm, 25 fs pulse duration with 2 mJ maximum energy per pulse at 1 kHz repetition rate. Two mechanical shutters (Vincent tech. Inc. USA) of 6 mm aperture are placed in the beam path. Both the shutters are individually operated through a shutter controller and their opening and closing times are triggered by the incoming pulse train. The electronic delay of both the shutters is compensated using the SRS delay generator. The system is set such that by pressing a switch, one can operate one cycle of the double-shutter system. The transmitted pulse is monitored on an oscilloscope by a fast Si photodiode (PD).

Figure1(b) demonstrates clean isolation of single fs pulse from the input pulse train at 1 kHz. The shutter S1 is open, while S2 is closed. The electronic trigger signals for both the shutters are shown with a sub-ms time delay transmission window which allows only one pulse to go through the double-shutter system as shown by the PD signal recorded on the oscilloscope. It is worth mentioning that while individual shutter offered minimum 1.3 ms total opening time, with DSG, we created sub-ms transmission window that allowed us to cleanly extract a single fs pulse.

Moreover, we varied the delay between opening and closing of two shutters to precisely extract multiple pulses from the fs pulse train. For example, Fig. 2(a) shows isolation of N=1 to 5. The intensity in each pulse remained constant. We have tested that the number of transmitted pulses can be increased one by one up to a large number.

In addition, DSG technique can be repeatably operated at variable cycles in order to control the repetition rate of the input pulses. We reduced the pulse repetition rate from 1 kHz down to 25 and 12.5 Hz without altering the original configuration of the laser systems (Fig. 2b). In our setup, the chosen shutters sustained multiple operation cycles with low vibrations and heat dissipation. The damage threshold of the metallic shutter blades is about 5 W/mm^2 which is much higher compared to the 6 mm beam size

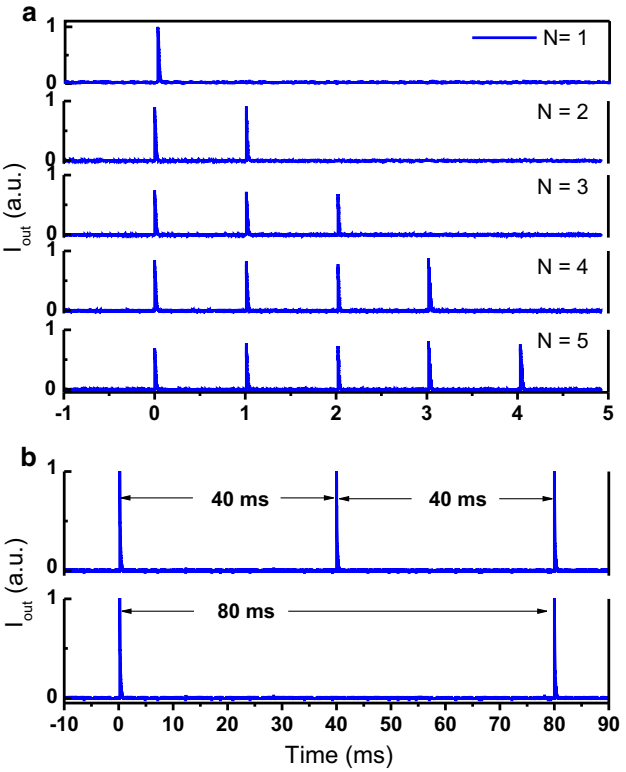

Fig. 2 (**a**) The photodiode signal showing extraction of N=1 to 5 pulses. (**b**) Repeated operation of double-shutters with single-shot selection window at two time intervals of 40 ms and 80 ms. The repetition rate of the input pulses was reduced from 1 kHz down to 25 Hz and 12.5 Hz without altering the original configuration of the laser systems

(0.1 W/mm^2). Table 1 compares the DSG technique with existing commercial and homemade shutter systems [18–24]. The DSG technique offers a much smaller transmission window that can be finely tuned.

4. Results and discussion

4.1. Plasma ablation of silicon

The ease and reliability of double-shutter system allowed us to perform single fs pulse processing. In order to physically confirm the single fs pulse ablations on a silicon wafer (<100>, N-type Sigma-Aldrich), the beam is focused through 20× (NA: 0.2) objective. The applied pulse energies at the sample surface are 1 μJ and 10 μJ [Fig. 3(a), (b)]. The sample is exposed to 1, 2, 5, 10, 25 and 50 pulses. After irradiation, the surface is cleaned ultrasonically for about 30 min and SEM micrographs are taken without any coatings as shown in Fig. 3. From SEM image of single-pulse ablation at lower energy, one can predict that the beam shape is circular and no distortion is

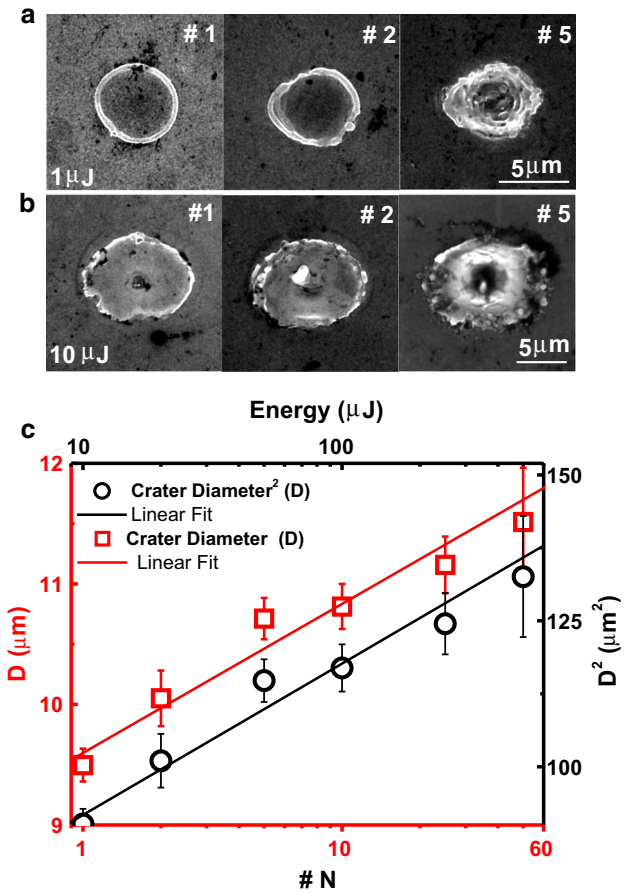

Fig. 3 Variation of the crater diameter D as a function of N on Si wafer. The applied pulse energies Si surface were (**a**) 1 μJ and (**b**) 10 μJ, respectively. (**c**) Semilog plot of D versus N for 10 μJ energy (red squares) and D^2 values is plotted to determine the threshold ablation energy and Gaussian beam radius

introduced after passing through the shutters. With an increase in the number of pulses, various nonlinear phenomena are accommodated that play a role in increment of crater size, plasma-assisted ablations could be one of them[1, 15, 33].

From SEM micrographs, the crater size is quantified as a function of the number of pulses and applied energy E. Figure 3(c) illustrates the increase in the crater diameter D with the number of pulses N. The clean microstructure produced by a single-shot appeared degraded with multiple shots due to accumulation effects. With increasing the applied energy per pulse from 1 to 10 μJ, an increase in crater size is observed. The increment is found to be linear with an increase in N [15, 34, 35].

To determine the ablation threshold energy as well as Gaussian beam radius over the dielectric surfaces, many different methods have been reported [36–38]. Applying laser pulses with a Gaussian beam profile, a relation between the crater diameter D, and maximum laser energy E_0, can be expressed as $D^2 = 2w^2 \ln[E_0/E_{\text{th}}]$, where E_{th} and w denote the ablation threshold energy and the $1/e^2$ Gaussian beam radius, respectively [32, 34, 39]. Figure 3(c) shows the semilogarithmic plots of the square of an ablation diameter D as a function of the energy. A linear dependence can be clearly identified. At a lower laser energy, a fit of the semilogarithmic plot of D^2 versus E_0 to experimental data gives $w = 2.4 \pm 0.1$ m and $E_{\text{th}} = 2$ nJ (corresponding fluence, 0.01 J/cm^2). The estimated beam spot radius is in agreement to the theoretical value of 2. 5 μm that is estimated by using the equation $w = 2\lambda/\pi NA$. The ablation threshold (E_{th}) for multiple pulse exposures is lower than the reported values [39–41]. It is probably due to energy accumulation effect at the vicinity of focal volume [2, 15].

4.2. Nanoscale ablation of silk

We measured a single-shot response of spider silk fiber of about 2–3 μm in diameter [42, 43] (Fig. 4). It is positioned at the focus using 100x objective (NA: 0.9) with an estimated beam spot size around 1 micron. SEM micrographs illustrate the single-pulse ablation of silk fiber at 0.1 μJ and 0.3 μJ pulse energies. The estimated ablation threshold (E^s_{th}) for spider silk is about 0.05 μJ (1 J/cm^2). A slightly lower ablation threshold (0.6 J/cm^2) for silkworm silk is reported for different laser parameters with 230 fs pulses at the central wavelength of 515 nm wavelength [44]. This could be due to differences in the laser parameters as well

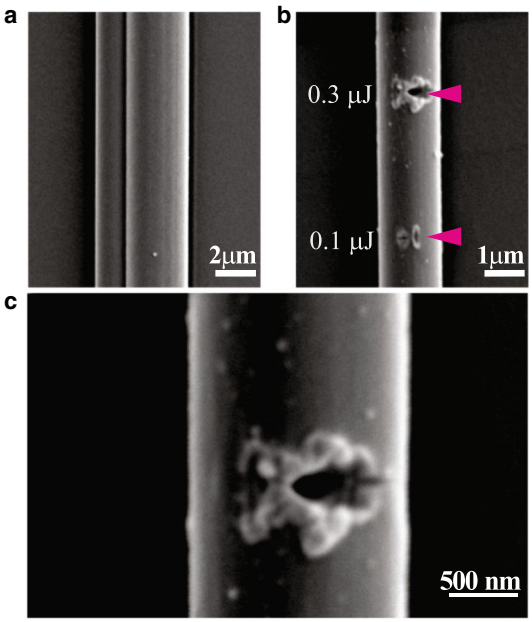

Fig. 4 (**a**) Native spider silk. (**b**) Illustrating ablation of silk fiber at different pulse energies 0.3 and 0.1 μJ, and (**c**) Magnified SEM micrograph illustrating nanoscale ablation of spider silk microfiber at 0.3 μJ

as the material properties [35, 39, 43]. E_{th}^{s} is found to be significantly higher than ablation threshold for the crystalline *Si*, it could be attributed to the non-absorbing nature of silk sample for incident laser wavelength, i.e., 800 nm [33, 35]. By compensating the dispersion of the fs pulse, it should be possible to further reduce the precision of ablation and may open route to create nanopatterns on silk for various potential applications.

4.3. Transient response of Agarose gel

We measured the single-shot transient response of 1-mm-thick agarose gel, prepared by standard technique [31]. The microscope surface images are recorded using a fast CCD camera (see inset of Fig. 5 for crater images at 0.0, 0.03 and 1.0 ms time delay) after exposure of a single laser pulse with 50 μJ energy on gel surface. In less than 0.1 ms, the crater diameter has reached its maximum value of about 24 ± 1 μm, which exponentially relaxed slowly. After 2 ms, the crater size became constant around 18.5 μm [45]. We observe about 6 μm change in crater diameter in 2 ms time, showing the possibility of two successive pulses in the pulse train may interact with the material rather than a single fs pulse. Such residual mechanical deformation may increase the roughness of the treated surface if processed at 1 kHz rep rate. Therefore, in fs laser-assisted cutting/dissecting operations, it is essential to optimize inter-pulse intervals by taking into account the intrinsic relaxation of the material by single fs pulse [1, 31, 45].

We would like to mention a couple of remarks regarding the DSG technique. (1) The setup can be made fully automated and compact where the delay generator could be replaced with software control. (2) Our technique can be operated under a high vacuum condition to cleanly isolate XUV or electron pulse(s). (3) It can also work with MHz pulses, if the input beam diameter can be reduced, e.g., by placing the two shutters near the focus. This suggests many practical applications of DSG technique to study single-shot phenomena.

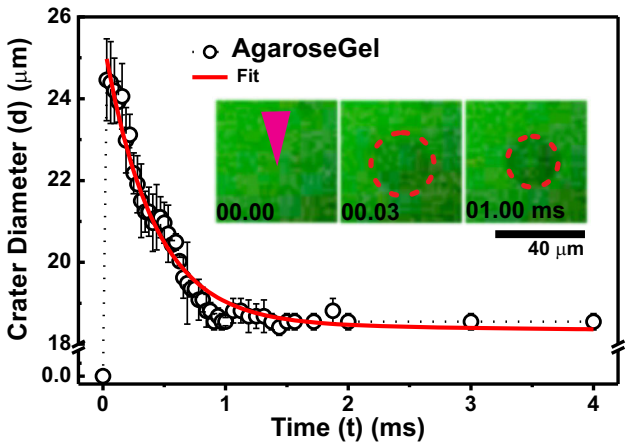

Fig. 5 Transient change in crater diameter on single fs pulse exposure (0.05 μJ) on 1-mm-thick agarose gel (1 %) surface. The experimental data of change in crater diameter can be fitted by an exponential function ($d = 18 + 7.0\ e^{-t/0.4} + 0.3\ e^{-t/11} + 0.2\ e^{-t/15}$) with three different relaxation time constants as shown in the fit equation

5. Conclusion

In conclusion, we demonstrate that the double-shutter gating technique provides a simple solution to the important problem of cleanly selecting a single fs pulse from a 1 kHz pulse train. By placing two identical shutters in the beam path and controlling their opening and closing time, we generated a tunable transmission window which is much smaller compared to a single shutter. Besides cleanly isolating the single fs pulse, we also extracted the desired number of fs pulses ($N = 1, 2, 3, \ldots$) from a 1 kHz pulse train. Both the photodiode signal and fs ablation of Si confirmed a clean selection of light pulses with clear differences between single and multiple shot response. This technique could also be used to optimize fs laser parameters for precision processing of viscoelastic materials (skin, tissues) by measuring their slow transient response after interaction with a single fs pulse. The DSG setup is compact, portable and can be easily inserted in the beam path without altering laser configurations to study single fs pulse phenomena. We envisage applications of DSG technique in determining single-shot damage threshold of materials, material processing, time-resolved spectroscopy with fs pulses and in extracting short pulses of XUV or electrons.

Acknowledgements We thanks I. Singh for SEM images of crystalline silicon surface and central SEM facility for imaging silk. We acknowledge DST and Max Planck Society for financial support.

References

[1] C B Schaffer, N Nishimura, E N Glezer, A M T Kim and E Mazur *Opt. Exp.***10** 196 (2002)
[2] H Gandhi, E Mazur, K Phillips and S K Sundaram *Adv. Opt. Photon.* **7** 684 (2015)
[3] M Malinauskas, A Zukauskas, S Hasegawa, Y Hayasaki, V Mizeikis, R Buividas and S Juodkazis *Light: Sci. Appl.* **5** e16133 (2016)
[4] N Düdovich, O Smirnova, J Levesque, Y Mairesse, M Yu Ivanov, D M Villeneuve and P B Corkum *Nat. Phys.* **2** 781 (2006).
[5] Z Chang *Fundamentals of Attosecond Optics* (CRC Press, London, 2011)p.1
[6] J C Hebden, R A Krüger and K S Wong, *Appl. Opt.* **30** 788 (1991)

[7] J C Dean, S R Rather, D G Oblinsky, E Cassette, C C Jumper and G D Scholes, *J. Phys. Chem. A* **119** 9098 (2015)
[8] T Brixner, T Pfeifer, G Gerber, M Wollenhaupt and T Baumert *Femtosecond Laser Spectroscopy* (Springer, New York, 2005)p.225
[9] L Stebbings, F Sübmann, Y Y Yang, A Scrinzi, M Durach, A Rusina, M I Stockman and M F Kling *New J. Phys.* **13** 073010 (2011)
[10] S Wyatt, T Witting, A Schiavi, D Fabris, P M Hernando, I A Walmsley, J P Marangos and J W G Tisch, *OPTICA* **3** 303 (2016)
[11] B Rethfeld, D S Ivanov, M E Garcia and S I Anisimov, *J. Phys. D Appl. Phys.* **50(19)** 193001 (2017)
[12] N Götte, T Kusserow, T Winkler, C Sarpe, L Englert, D Otto, T Meinl, Y Khan, B Zielinski, A Senftleben, M Wollenhaupt, H Hillmer, and T Baumert Temporally shaped femtosecond laser pulses for creation of functional sub-100 nm structures in dielectrics. In: König K, Ostendorf A (eds.) *Optically Induced Nanostructures: Biomedical and Technical Applications* (Berlin: De Gruyter) Chapter 3 (2015)
[13] J Wentz Polarization Independent Light Modulation Means Using Birefringent Crystals, U.S. patent 3,719,414 (1973)
[14] http://www.thorlabs.com/ for Electro-Optic Modulators (last accessed 13 Apr 2018)
[15] F D Niso, C Gaudiuso, T Sibillano, F P Mezzapesa, A Ancona and P M Lugara, *Opt. Exp.* **22** 12200 (2014)
[16] U K Tirlapur and K König *Nature* **418** 290 (2002)
[17] A Roberts, D Cormode, C Reynolds, T Newhouse-Illige, L J Brian and A S Sandhu, *Appl. Phys. Lett.* **99** 051912 (2011)
[18] http://www.thorlabs.com/ for Optomechanical Devices SH05, http://www.uniblitz.com/ for Optical Shutters LS56, and http://www.thinksrs.com for Laser shutters and controllers SRS470 and SRS474 (last accessed 13 Apr 2018)
[19] D M Mills, *Rev. Sci. Instrum.* **60** 2338 (1989)
[20] M Gembicky and P Coppens *J. Synchroton Rad.* **14** 133 (2007)
[21] D Kosciesza and H D Bartunik *J. Synchroton Rad.* **6** 947 (1999)
[22] R Tucoulou, D V Roshchupkin, O Mathon, I A Schelokov and M Brunel, *J. Synchroton Rad.* **5** 1357 (1998)
[23] A McPherson, W K Lee and D M Mills, *Rev. Sci. Instrum.* **73** 2852 (2002)
[24] M Ye and D Jiang *Rev. Sci. Instrum.* **61**, 2003 (1990)
[25] C S Adams, *Rev. Sci. Instrum.* **71** 59 (2000)
[26] L P Maguire, S Szilagyi and R E Scholten, *Rev. Sci. Instrum.* **75** 3077 (2004)
[27] S Zhang and G Wilson Practical method and device for enhancing pulse contrast ratio for lasers and electron accelerators, U.S. patent 8,842,703 (23 September 2014)
[28] P Coppens, I Vorontsov, T Graber, M Gembicky and A Y Kovalevsky, *Acta Cryst. A* **61** 162 (2005)
[29] K Kawase, R Kato, A Irizawa, M Fujimoto, K Furukawa, K Kubo and G Isoyama *Proc. of FEL 2015*, (Daejeon) pp 430–432 (2015)
[30] G Romo-Cárdenas, F G Péerez-Gutiérrez , A Mina-Rosales, S Camacho-López, G Aguilar *AIP Conf. Proc.* (2006)
[31] F G P Gutiérrez, S Camacho-Lóopez, and G Aguilar, *J. Biomed.Opt.* **6(11)** 115001 (2011)
[32] M S Sidhu PhD Thesis (University of Science and Technology, Daejeon, Rep. of Korea) (2014)
[33] C B Schaffer, A O Jamison, J F Garcia and E Mazur *Ultrafast Lasers: Technology and Applications* (Marcel Dekker Inc. New York) p 395 (2002)
[34] A B Yakar and R Byer *J. Appl. Phys.* **96** 5316 (2004)
[35] A Vogel and V Venugopalan *Chem. Rev.* **103** 577 (2003)
[36] J. M. Liu, *Opt. Lett.* **7**, 196 (1982).
[37] M A de Araújo, R Silva, E de Lima, D P Pereira and P C de Oliveira, *Appl. Opt.* , **48** 393 (2009)
[38] G Tsigaridas, M Fakials, I Polyzos, P Persephonis and V Giannetas, *Appl. Phys. B* **76** 83 (2003)
[39] S Preuss, A Demchuk and M Stuke, *Appl. Phys. A* **61**, 33 (1995)
[40] J Bonse, S Baudach, J Kruger, W Kautek and M Lenzner, *Appl. Phys. A* **74** 19 (2002)
[41] H O Jeschke, M E Garcia, M Lenzner, J Bonse, J Krüger and W Kautek, *Appl. Surf. Sci.* **197-198** 839 (2002)
[42] F Vollrath, B Madsen and Z Shao, *Proc. R. Soc. Lond. B* **268** 2339 (2001)
[43] M S Sidhu, B Kumar and K P Singh, *Nat. Mat.* **16** 938 (2017)
[44] M Ryu, H Kobayashi, A Balytis, X Wang, J Vongsvivut, J Li, N Urayama,V Mizeikis, M Tobin, S Juodkazis and J Morikawa, *Mater. Res. Exp.* **4** 115028 (2017)
[45] H Y Moon, M S Sidhu, H S Lee and S C Jeoung, *Opt. Exp.* **23** 19854 (2015)